Research Article

Jasmine Almond, Piriya Sugumaar, Margot N. Wenzel, Gavin Hill, and Christopher Wallis*

Determination of the carbonyl index of polyethylene and polypropylene using specified area under band methodology with ATR-FTIR spectroscopy

https://doi.org/10.1515/epoly-2020-0041
received February 18, 2020; accepted May 03, 2020

Abstract: The current measurement techniques described in the literature for the determination of the carbonyl index (CI) for polyolefins such as polyethylene and polypropylene were compared and contrasted. These were all found to be inconsistent or inaccurate and were not capable of differentiating significant changes in carbonyl peak evolution throughout accelerated ageing. As a consequence of these findings, a methodology, specified area under band (SAUB) is presented here to more accurately represent the CI as a general means of reporting. The increased precision in the methodology is explained and compared to other methodologies for determining CI. The SAUB method is also shown to be capable of elucidating the differences in relative extent and rates of CI for different polyolefins, exposed to the same conditions over the same time period.

Keywords: FTIR, carbonyl index, accelerated ageing, polyolefin, polyethylene, polypropylene

1 Introduction

Polyolefin materials, particularly polyethylene (PE) and polypropylene (PP), are susceptible to oxidation in the presence of air during long-term service. Oxidation may also be deliberately carried out during the manufacturing process, as a means of chain length control, or surface modification such as corona treatment (1,2). This process causes significant changes in not only the chemical structure of the material but the physical properties of the material as well. The oxidation of polyolefins can be monitored through a series of different methods such as thermal analysis by differential scanning calorimetry, rheology, tensile properties and excitational/vibrational spectroscopy as a few examples. One of the most common analytical techniques to monitor oxidation reactions is Fourier transform infrared (FTIR) spectroscopy to observe changes in the carbonyl band (C═O) which has given rise to a method called the carbonyl index (CI) (3,4). FTIR analysis is capable of monitoring other chemical changes that take place throughout the lifetime of a material, by detecting the functional groups present at distinct bands. The CI is used to specifically monitor the absorption band of the carbonyl species formed during photo or thermo-oxidation processes in the range of 1,850–1,650 cm^{-1}, by measuring a ratio of the carbonyl peak relative to a reference peak. Not only is the CI used to measure oxidation occurring throughout the lifetime of polyolefins, but it is also employed to predict their service life and to develop stabilisation additives for materials (5,6). Additionally, the CI is deployed as a tool to monitor surface modifications as a function of new carbonyl species present, where targeted oxidation such as ozonolysis may be carried out through processes such as copolymerisation (7).

For the last 45 years (3,4), the CI has been studied and recorded as a common way of monitoring this physicochemical change; however, there is no current universal method for determining CI. Indeed, when looking into the literature, a multitude of different methods are reported. Table 1 demonstrates a few different examples of the calculation methods used and their corresponding references. With so many different variations in measuring CI, comparison of the results seems to be impossible and meaningless, as the various methods produce CI values on completely different scales (Table 1). These variations make it difficult to determine what value of CI equates to a significant level of oxidation for a polyolefin material. This issue was the starting point for this study, which was carried out to develop a CI method that could be used universally to reduce error and provide consistent and comparable results across different polyolefin materials. The various methods reported in the literature were initially compared to determine the accuracy and reliability of the results and, as predicted, the majority of

* **Corresponding author: Christopher Wallis,** Polymateria Limited, Translation and Innovation Hub, Imperial College White City Campus, 80 Wood Lane, White City, London, UK, e-mail: cw@polymateria.com
Jasmine Almond, Piriya Sugumaar, Margot N. Wenzel, Gavin Hill: Polymateria Limited, Translation and Innovation Hub, Imperial College White City Campus, 80 Wood Lane, White City, London, UK

Table 1: Selection of the different CI methods previously reported and their corresponding references

	Description of methodology	Instrument method	Specified wavenumbers (cm^{-1}) (CI = *X*/*Y*)	Material	Range of CI values	Reference
1	Ratio absorbance height	Transmission FTIR	1,714/720	PE (100 µm)	0–1.2	(10)
2	Ratio of maximum absorbance height	Transmission FTIR	1,720/720	PE (36 µm)	0–2.5	(5)
3	Ratio of absorbance height	Transmission FTIR	1,713/730	PE (45 µm)	0–1.6	(11)
4	Ratio of absorbance height	Transmission FTIR	1,710/1,380	PE (20–30 µm)	0–2	(12)
5	Ratio of absorbance height	Transmission FTIR	1,714/1,463	PE (14 µm)	0–0.8	(13)
6	Average absorbance area of carbonyl peak over reference ATR-FTIR	Absorbance ATR-FTIR	1,700–1,780/1,463	PE (25–76 µm)	0–0.8	(14)
7	Ratio of absorbance height (keto carbonyl index)	Not published	1,714/1,462	PE 2 mm	0–0.4	(15)
8	Ratio of absorbance area PE-polymer band	Absorbance ATR-FTIR	1,714/147	PE (60 µm)	0–1.2	(16)
9	Ratio of absorbance height	Absorbance ATR-FTIR	1,712/1,472	PE (50 µm)	0–1.1	(17)
10	Ratio of absorbance height	Transmission FTIR	1,740/2,020	PE (70 µm)	0–15	(18)
11	Ratio of absorbance area	Absorbance ATR-FTIR	(1,850–1,630)/(peak at 1,380 PE) or (peak at 2,700–2,750 PP)	PE + PP (various)	0–1.3	(19)
12	Subtraction of baseline	Absorbance ATR-FTIR (Ge)	1,751–1,895	PE + PP (unknown)	0–0.8	(20)
13	Ratio of absorbance maximum height within given ranges	Not published	1,708–1,720/1,880–1,910	PP (500 µm)	2.5–20	(21)
14	Ratio of absorbance height	Transmission FTIR	1,725/2,722	PP (30 µm)	0.25–0.60	(22)

them show inconsistencies. Based on the findings in this report, it is the opinion of the authors that to develop a standard, one methodology should be chosen from the field below. In this case, the authors favour the use of the specified area under band (SAUB) method, for use with attenuated total reflection (ATR)-FTIR spectroscopy, as the most effective method of determining the CI.

In the last 20 years or so, ATR-FTIR spectroscopy and its variants have largely superseded transmission measurements as the main method of obtaining infrared spectra measurements for a range of materials. ATR-FTIR spectroscopy has distinct advantages in sample handling, in that it is a non-destructive method that requires little-to-no sample preparation. While FTIR measurements in transmission work well for thin films, eventually saturation takes place leading to a distorted baseline and broadening of the peaks. For thicker materials, however, transmission measurements are not possible. In addition, when materials are being evaluated while undergoing artificial or natural weathering (one of the main purposes for CI determination), any embrittlement that can occur during the process makes measurements more difficult.

ATR-FTIR spectroscopy, on the other hand, is a surface technique and works through a process of passing light through a crystal in contact with the sample. If the difference in refractive index between the crystal and sample is high enough, then an effervescent wave forms penetrating into the sample before being reflected back out to the detector. The depth of penetration is dependent on the IR wavelength and refractive index of the sample, and signal intensity is affected by the contact between sample and crystal and number of bounces, which in turn is related to the angle of incident light. For most organic materials on a diamond or zinc selenide surface, a 45° incident angle is the standard setup for most ATR-FTIR accessories, this is standard for a single bounce method, where the emission from the evanescent wave exits also at 45° and the depth of penetration is up to 2 µm. Multi-bounce ATR platforms are also available in which the incident angles can be between 19° and 45° (8), where the wave travels a longer path and has a different penetration depth. This technique creates multiple evanescent waves, and these are often utilised for the study of plastic additives as they enhance some of the weaker signals in the spectrum. Based on all the factors highlighted above, we selected ATR-FTIR spectroscopy as the preferred measurement technique to determine the CI of PE and PP samples.

There is a growing interest in the impact of plastic materials in the natural environment, with an increasing number of academic and national laboratories now focussed on reviewing current and developing new methodologies for the identification of plastic and microplastic materials. These

materials are migrating from terrestrial disposal routes into the watercourses and oceans, with finer particles and fibres even being found in the air. This is leading to a greater awareness of the role that weathering plays in misidentification of plastic materials exposed to the natural environment for indeterminate time periods (9). While techniques such as Raman spectroscopy are starting to come to the fore in aiding in the identification of plastic and microplastic materials, the role of FTIR and ATR-FTIR will remain central owing to its ease of use, low cost and sensitivity. ATR-FTIR is one of the best and least destructive methods in that little-to-no sample preparation is required. Samples can thus be identified rapidly using the sensitivity of the functional group analysis or existing libraries of spectra. Therefore, standardising the methodologies around identifying materials is of paramount importance. Equally so is the introduction and familiarisation to the next wave of researchers of the issues around environmental oxidation and the role of assessing CI. This is instrumental in the development of new standards and metrology for the identification of plastic materials, in the natural environment, or any materials that will react in an oxidative environment.

2 Experimental

2.1 Materials

The 1-butene linear low-density polyethylene (LLDPE) (Borstar FB2230) used in this study was supplied by Borealis, and the information provided by the manufacturer states: a high molecular weight, melt flow rate (ISO 1133) of 0.2 g/10 min (190°C/2.16 kg) and a density (ISO 1183) of 923 kg/m^3, and it contains an unspecified antioxidant. The isotactic PP homopolymer (PPH 11012) used in this study was supplied by total petrochemicals, and the information provided by the manufacturer states: a nucleated controlled-rheology antistatic homopolymer, with a melt flow index (ISO 1133) of 55 g/10 min (230°C/2.13 kg) and a density (ISO 1183) of 0.905 g/cm^3, and it is likely that this material contains undisclosed amounts of primary and secondary anti-oxidants, as well as an undisclosed anti-static additive.

2.2 Methods

2.2.1 Production of test specimens

For the LLDPE resin, clear film samples were blown on a Collin film blowing line, at Norner AS (Norway). The screw speed was set to 70 rpm and a temperature profile of 190°C–199°C was used. The blow-up ratio was a maximum of 3 producing a final film with a thickness of 20 μm. The film was cut into 14 cm × 2.5 cm strips to be used for accelerated ageing.

The PP resin was used to make injection moulded strips (80 mm × 10 mm × 1 mm) using an ENGEL CC90 injection moulding machine, at Norner AS (Norway). The machine had a screw diameter of 35 mm and an L/D of 17. The conditions for the injection moulding included a melt temperate of 200°C, a mould temperature of 40°C and an injection speed of 50 mm/s.

2.2.2 Photo-oxidation

Both the blown LLDPE film and injection moulded PP test samples were subjected to artificial accelerated ageing conducted in a QUV tester (Q-Labs, USA). The tester was fit with UVA lamps calibrated at 340 nm and programmed to follow the ASTM D5208 standard (23) under cycle C, which consists of a dry cycle set at a temperature of 50°C with a continuous irradiance of 0.89 W/m^2. The test was run for a total of 28 days with samples removed every 3 or 4 days to monitor the oxidation occurring by FTIR analysis.

2.2.3 Thermooxidation

LLDPE film samples were subjected to thermal accelerated ageing at 60°C in an air-circulated oven. Samples were removed periodically and analysed to measure the oxidation occurring by FTIR analysis.

2.2.4 Infrared spectroscopy (FT-ATR)

Infrared spectra were obtained using a Nicolet iS5 (Thermo Fisher Scientific) equipped with an ID7-ATR spectrometer with a diamond crystal with a fixed incident angle of 45°. The specimens were analysed in triplicate by absorbance spectra in the region between 4,000 and 400 cm^{-1}, with 32 scans at 4 cm^{-1} resolution using OMNIC software by Thermo Fisher Scientific. These were chosen as standard parameters that the majority of InfraRed spectrometer can run.

2.2.5 Calculation of the SAUB CI

The CI was calculated from the ratio between the integrated band absorbance of the carbonyl (C=O)

peak from 1,850 to 1,650 cm^{-1} and that of the methylene (CH_2) scissoring peak from 1,500 to 1,420 cm^{-1} as expressed in the following equation:

$$\text{Carbonyl index (CI)} = \frac{\text{Area under band 1,850–1,650 cm}^{-1}}{\text{Area under band 1,500–1,420 cm}^{-1}}. \quad (1)$$

The limits for the baseline are chosen using data from the $T = 28$ measurements, as this has the highest variability and is fitted on the Omnic software, so each sample uses the same parameters. However, a flat baseline can usually be taken from data between 4,400 cm^{-1} and 2,000 cm^{-1}. While it can be expedient to take the baselines immediately at the limits of the individual peaks or to correct the baselines using software correction, this has been avoided as it can potentially skew the outcome of the CI measurements. The CI is taken as the average of at least three random samples from the test material and test area.

The area under the band is calculated through the Omnic software options using the peak analysis tool. This allows the user to select the baseline limits and enter the limits for the spectrum. This feature is available on most modern IR spectrophotometers.

3 Results and discussion

3.1 A comparative review of ATR-FTIR collection modes from the literature

As this section highlights, it is often difficult to compare measurements of CI taken from different publications; however, it is possible to review each methodology on its own merits and to suggest which methodology may have been better used. For the measurement of thin films FTIR spectra in the transmission mode will give useful data, but eventually the quality of the results will be impacted by saturation of the bands. Most groups represent this by using the reciprocal of the transmittance, absorbance, as this tends to improve the baseline resolution. This in turn creates issues around the baseline, which should not be altered when trying to do any quantitative assessment, as it can be difficult to reproduce and can be used to adjust the outcome. There is no defined maximum thickness for the film, as this will depend somewhat on the physical appearance of the film. An opaque film, for example, will absorb or scatter more light and therefore will limit this technique to thinner films. Method 1 from Table 1 (10), where an LLDPE and LDPE film containing a pro-oxidation catalyst was thermally aged as described in Section 2.2.3. The resulting transmission FTIR spectra on 100 µm films with minor baseline correction, the C–H stretching bands at 2,900 cm^{-1} were saturated, indicating that the film was too thick for meaningful transmission mode measurements. As a result, the authors had to use the 720 cm^{-1} resonance band as a reference peak instead. By 30 days of accelerated aging, the C═O band had broadened and saturated to such a degree that a plateau instead of peak was observed in the spectrum, and thus, the last meaningful data point collected to determine the CI was at 15 days, clearly demonstrating the limitation of this method of measurement.

Alternatively, the use of ATR-FTIR spectroscopy would have shown improved signal and baseline resolution; however, the 720 cm^{-1} band would not be recommended as a reference band in ATR, as the intensity of peaks is less consistent across the whole spectrum. Improved consistency in the peak intensity occurs when bands are chosen within a few 100's of wavenumbers. Therefore, while it may be desirable to use the FTIR transmission mode due to hardware availability or method familiarity, for measuring CI determination of the range of materials to which it can be applied is very limited. While it can be argued that materials can be pressed into thinner films for transmission measurements, this could only be considered prior to the aging of the material. The reasons are that many of the fundamental physical properties of a thermoplastic polymer exist as a result of the manufacturing process. Therefore, erasing this thermal history can fundamentally change the microcrystalline structure of the test material, increase migration of additives to the interface and even result in loss of volatile carbonyl species.

Method 2 which is similar to method 1 (Table 1) by Focke and co-workers (5) used a 40 µm film, aged similar to the methods described in Section 2.2.2 and produced results without band saturation, due to the choice of sample being a thin and clear film.

The most problematic aspect of several methods used to determine a CI listed in Table 1 was that the authors did not state whether it was FTIR or ATR-FTIR spectroscopy that was used. This is unfortunately symptomatic of the current state of the art of CI determination and is a result of the lack of a standardised methodology. Without reporting this key piece of information, it raises questions as to the validity of their determined CI. As an example, Tocháček and Vrátníčková (21) prepared PP plaques of 500 µm thickness and determined their CI using FTIR spectroscopy

in the transmission mode. There are no spectra shown in their publication, and it is the opinion of these authors that it is not possible to measure a CI using FTIR spectroscopy in the transmission mode at such a high thickness of polyolefin sample. In fact, upon comparing all the methods run on PE films, most films had thicknesses less than 50 µm, indicating that this may be a good ceiling thickness after which transmission FTIR spectroscopy should not be considered a viable technique for determining the CI of the polyolefin material.

3.1.1 Improved precision using SAUB compared to peak height measurements

It is the opinion of the authors, and it will be demonstrated in the following sections that determination of the CI using the SAUB technique increases the level of precision through consideration of all species present and avoiding user error when choosing which peak absorbance height to use. The peak area can simply be considered as a series of overlapping height bands and giving proper assignments to the complex series of peaks can often be beyond the capabilities of operator and can be open to different interpretations. This is crucial due to the complexity of species produced during oxidation and can represent carbonyl species that are chain terminating, within the main chain, and/or contained in newly generated oligomers and small molecules (MW < 300 Da). Furthermore, the bands corresponding to each carbonyl species often overlap in the spectrum, causing a broadening of the peak, which will result in a shortening of the overall signal. Thus, a broad "short" signal can have the same total area under the band as a sharp "tall" signal. To demonstrate this, PE samples PE 1 and PE 2 underwent photo-oxidation and thermal oxidation, respectively, and were analysed using ATR-FTIR spectroscopy (Figure 1 and Table 2). The IR spectra were recorded at three random points on the test material and the average of these values reported. For methods 4 and 5, values of 0 were returned at $T = 0$, while the SAUB method and method 12 recorded values that could be attributed to the presence of an undisclosed anti-static additive. Variance alone in the values obtained at each time point is not a good indicator as to the reproducibility of the method. Weathering, even under controlled conditions, may not happen uniformly across the sample, as degradation may take place faster at defects, points of stress, areas of low or high anti-oxidant levels or edge exposure. While all possible steps have been taken to ensure the quality of the samples produced and tested – it is one of the applications of the CI to determine the quality of a sample.

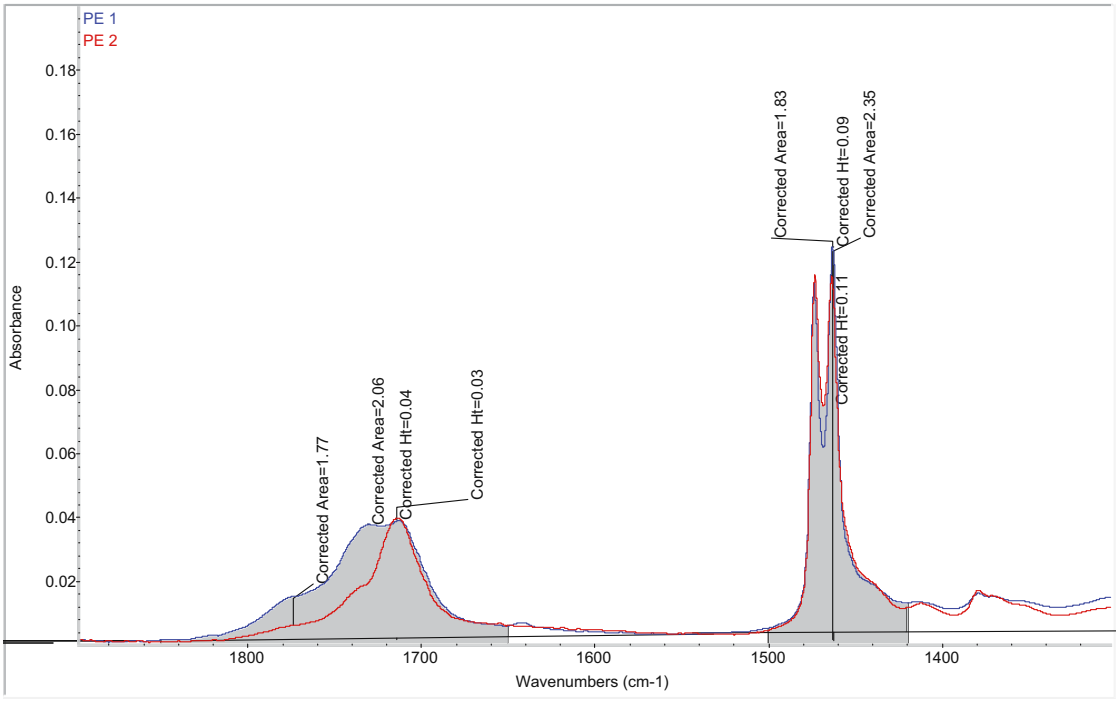

Figure 1: ATR-FTIR spectra of PE samples after having undergone accelerated ageing. The blue line corresponds to the ATR-FTIR spectrum of PE 1, which was exposed to thermooxidation, the red line is the ATR-FTIR spectrum of PE 2, which was exposed to photo-oxidation (at 340 nm).

Table 2: Comparison of the CI calculated using peak height or the SAUB method for a PE sample

Sample	Method of oxidation	CI average using peak height ($A_{1,714}/A_{1,463}$) (11)	CI average using the SAUB method
PE 1	Photo-oxidation	0.33	1.13
PE 2	Thermooxidation	0.36	0.75

Using the peak height measurement, which focuses on the wavenumber 1,714 cm^{-1}, the CI of PE 2 was greater than the CI of PE 1, as shown in Table 2. However, when looking at the spectra, although the PE 2 carbonyl band has a slightly higher intensity at 1,714 cm^{-1}, it is a sharper peak in comparison to the carbonyl peak for PE 1, which is broader in size. The broadening of this band, in this particular example, suggests that a greater variation in carbonyl species has been produced by photo-oxidation when compared to thermooxidation.

Focussing on singular peak heights introduces some issues: if a single wavenumber is chosen to represent CI, then it raises the question as to whether this is always the same C═O species being measured. At a 4 cm^{-1} resolution, this band will be a composite of multiple carbonyl species. Running at a higher resolution of 1–2 cm^{-1} (which some spectrometers may struggle to replicate) can create greater noise interference in the C═O band rather than providing clarity. The other concern related to this approach is the weighting of specific bands over others. The integrated area of the C═O band will be influenced by the concentration of the C═O species present and, in turn, their relative concentrations. When looking at the CI calculated using the SAUB method, it gives a more balanced representation of the relative total concentration of carbonyl containing species and is thus reflected in a higher CI. The peak area is in effect the sum of all peak heights; therefore, peak heights are still heavily weighted in favour of the CI using SAUB. Investigators who are only interested in specific carbonyl containing species are suggested to determine the "total" CI by peak area (preferably using the method described herein), followed by separate specific CI determinations for the individual peak heights of interest. While tools have been developed (24) to do peak deconvolution of overlapping peaks, this additional software comes at an added cost and is not easily implemented by all users.

3.1.2 Error occurrence and reduction of error associated with CI by the SAUB method

The rationale behind the choice of peak area measurement rather than intensity at a specific wavenumber is based on the fact that the breakdown of polyolefins does not produce solely ketones at 1,714 cm^{-1} but dozens of potentially different carbonyl products (25,26). These carbonyl species can be identified individually as γ-lactones (1,780 cm^{-1}), esters and/or aldehydes (1,733 cm^{-1}), ketones (1,714 cm^{-1})

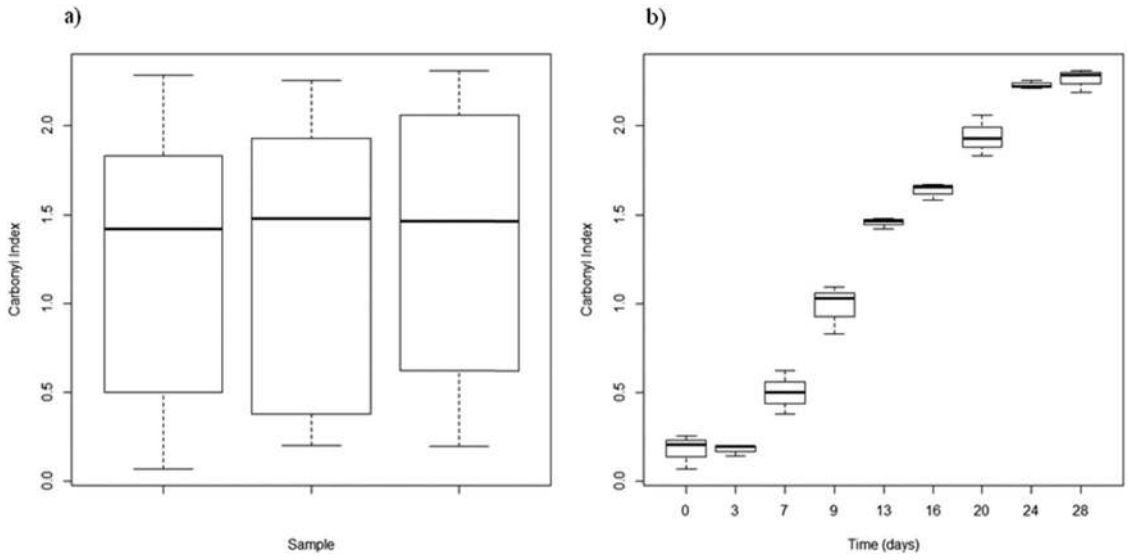

Figure 2: Box and Whisker plots of (a) CI variation in test replicates and (b) CI variations at each time point.

Table 3: CI calculations used to compare against the SAUB method

Method	Specified wavenumbers (cm^{-1})	Reference
12	1,751–1,895	(20)
4	1,710/1,380	(12)
10	1,740/2,020	(18)
5	1,714/1,463	(13)
SAUB	(1,850–1,650)/(1,500–1,420)	(This paper, 6)

and carboxylic acids (1,700 cm^{-1}) (16), and even these species do not have static peak assignments. It is also known that the peak position between ATR-FTIR and transmission FTIR spectroscopy often shifts slightly due to the change in refractive index. Many instrument suppliers provide a software correction for this, where the refractive index of the material and number of reflections are used as a correction versus the refractive index of the crystal. Therefore, using the SAUB technique in either FTIR or ATR-FTIR spectroscopy reduces any potential error due to shifting peak positions as the area under band will still account for this and be less influenced than any individual peaks within the bands. It is worth noting that the choice of common reference band becomes important when comparing data from ATR-FTIR and FTIR spectroscopy. Based on the reasons presented here, the authors suggest that when using ATR-FTIR spectroscopy, the best candidate for a reference band is either the CH bending modes for PE, or the CH_3 for PP, at between 1,500 and 1,420 cm^{-1} as the C–H stretching modes are most likely to saturate in transmission FTIR measurements. Additionally, this choice is advantageous over using the 720 cm^{-1} C–H bending vibrational mode as reference. The area between 1,500 and 1,420 cm^{-1} remains distinct throughout the degradation process – making it easier to measure and identify, while it is close enough to encounter similar levels of distortion due to contact changes or optical changes in the sample and thus the same baseline can be applied. As a sample degrades the resolution of the baseline changes, this is most apparent below 1,300 cm^{-1}, while few identifiable new peaks are observed in this region, the poor resolution can be attributed, in part, to the overlap of peaks arising from the number of possible chemical products containing C–O–C (1,300–1,000 cm^{-1}) and unsaturated C=C bonds (1,000–650 cm^{-1}) (26). The relative weakness of the 720 cm^{-1} peak makes it more susceptible to measurement error once baseline broadening effects due to overlapping C=C bending modes occur.

These parameters aid in reducing human error, as well as offsetting any potential differences in chemical composition of the by-products from oxidation of polyolefins. The advantage being proposed is that more accurate measurements can be made and thus subsequently compared to other test samples, to delineate and correlate the effect of different physical or chemical treatments upon the oxidation of polyolefins.

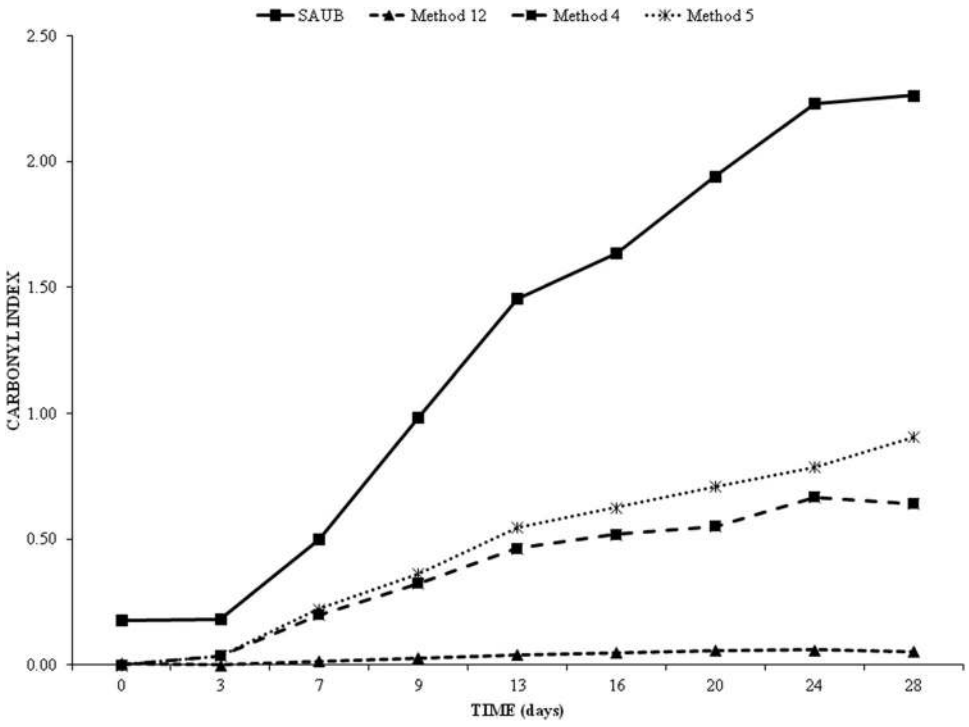

Figure 3: Plot of average CI vs. time for the different methods.

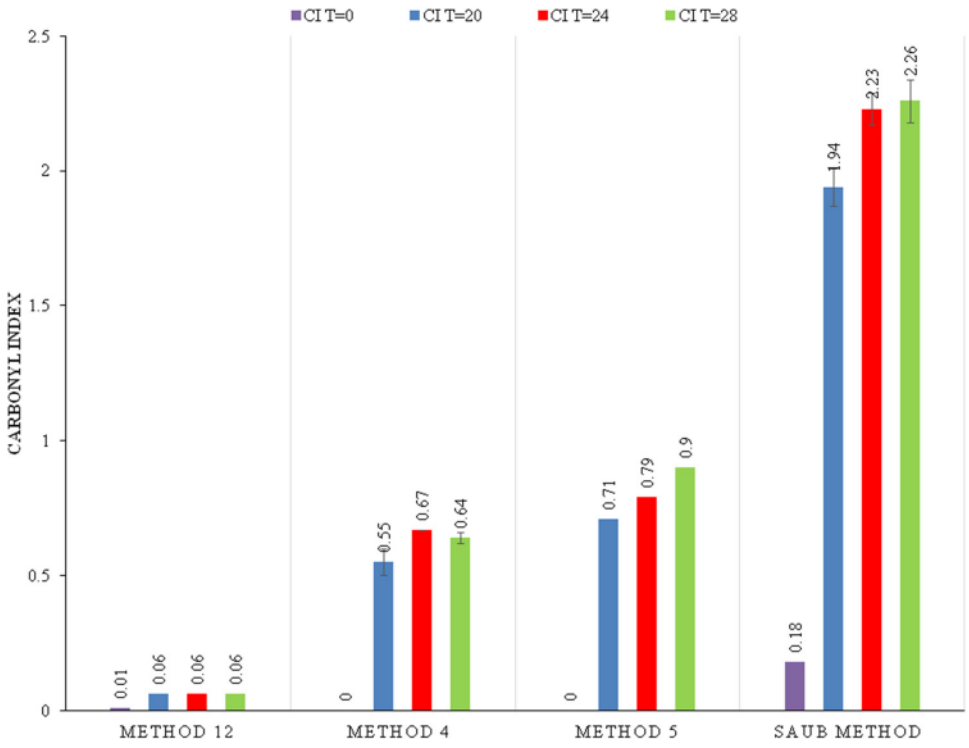

Figure 4: Average CI data of PP samples at $T = 0$ (purple), 20 days (blue), 24 days (red) and 28 days (green) of accelerated photo-oxidation, using the five different methods of calculation listed in Table 3. The error bars represent the standard deviation in the tests and the representative CIs are shown in the data labels.

A statistical analysis of the SAUB method was carried out by using analysis of variance (ANOVA) to assess the reproducibility of the CI of the sample taken. The test showed that there was no significant difference between the CI values across the three replicates (p value = 0.0694). Box and whisker plots were also prepared on a sample and time point basis (Figure 2a and b). These show that between the different samples recorded there is little variation in the mean for the values taken (in agreement with the ANOVA). The data recorded for specific time points over 28 days, however, showed a greater range of variations at each time interval, which we suggest reflects more on the differences in the relative degree of oxidation upon the points of the sample where the analysis was recorded, rather than on the precision of the method.

3.2 Comparison of the SAUB CI to other CI calculation methods

To demonstrate the effective accuracy of the SAUB method, the CI data produced using this method versus four of the other most commonly used peak height methods were compared. This comparison not only confirmed the increased accuracy in using a specified area versus peak height but also demonstrated that the changes in the carbonyl band can be accurately reflected over time as well. The methods compared are listed in Table 3.

Method 10, while being favoured by Andrady (3) and Roy et al. (18) as a method for determining CI is not applicable for ATR-FTIR as the 2,020 cm^{-1} thickness band chosen as a reference does not arise by this method. Given the data presented by Roy and co-workers, it is difficult to assess this peak as a choice for a reference band as the transmission FTIR spectrum, shown in their paper, suggested oversaturation of the C–H and C=O bands and poor baseline resolution; additionally, there are many examples of transmission PE spectra that do not contain any significant peaks at this wavenumber and this reference peak can appear in the range of 2,103–1,980 cm^{-1}, making it open to user interpretation.

The injection moulded PP samples which underwent photo-oxidation were used to compare the different methods of CI measurement (Figures 2 and 3). Figure 2 shows the evolution of the CI over the 28-day photo-oxidation period, where the differences between each method showed significant deviance. While it was clear

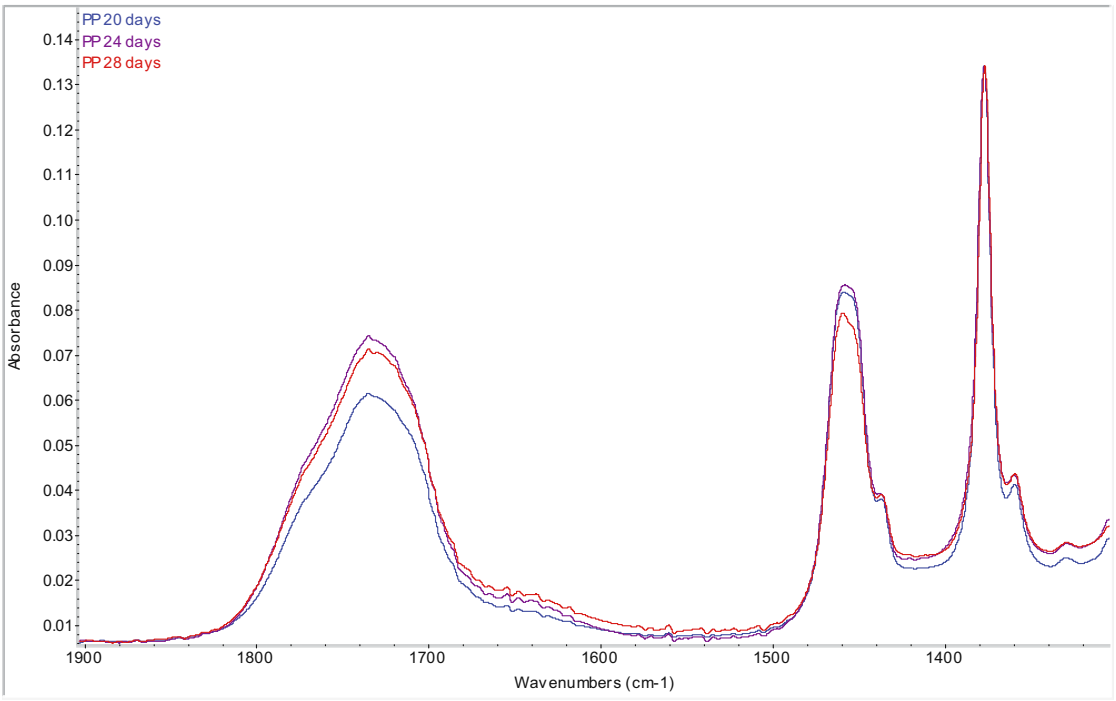

Figure 5: ATR-FTIR spectra in the region of 1,900–1,300 cm^{-1} of a photo-oxidised PP sample after 20 (blue line), 24 (red line) and 28 (black line) days of treatment.

from the data presented that there is a significant difference in the magnitude of the results of the SAUB method vs. the other methods, Dunnett's test was carried out using R software, with the SAUB method as the control versus methods 12, 4 and 5 across 28 days. The *p*-values for methods 12, 4 and 5 were 9.5×10^{-6}, 9.2×10^{-4} and 2.84×10^{-3}, respectively, which would lead to a rejection of the similarity hypothesis at the 1% level. Therefore, the outcomes of the SAUB method will almost always be different to the other methods, and the methods cannot be used interchangeably. This highlights the importance of identifying a universal method for the basis of standardised testing.

A comparison of the magnitude of the data from each method was recorded at time intervals of aging of 0, 20, 24 and 28 days (Figures 3 and 4). These intervals were chosen to ensure that a concise comparison could be made between all methods and allows for a subsequent comparison with PE, which has a longer photo-oxidation induction period (Figure 5).

The spectrum of the photo-oxidised PP sample clearly showed an evolution of the carbonyl region over time, especially between 20 and 24/28 days of UV treatment (Figure 3); however, this is not observed by all the calculated CI results (Figures 2 and 3). Methods 12 and 10 calculated the CI as remaining identical between 20 and 28 days of ageing; however, the ATR-FTIR spectra show a substantial difference between these intervals. This suggests that these two methods are not sensitive enough to be able to measure the smaller differences that occur in the oxidation process. Method 2 is inconsistent as it shows an increase in the CI to 0.67, followed by a decrease to 0.64. Only method 5 and the SAUB method reflect an accurate account of the change in CI over time for the PP sample. The SAUB method is a more precise representation of the changing CI as it accounts for the total concentration and variety of carbonyl containing species associated with the area under the band between 1,850 and 1,650 cm^{-1}. This compares to method 5, which relies upon a single peak height that relates only on the carbonyl species, predominately ketones, associated with the band at 1,714 cm^{-1}. Therefore, the SAUB method, in comparison to the other four methods evaluated, better indicates the overall change in CI over time, reflecting on the variance in species present.

The SAUB technique is equally viable for PE film samples, where transmission FTIR would normally be the chosen method. This allows for easier measurements, as heavily aged samples can be difficult to load into a vertical mounted spectrometer. To demonstrate this, blown LLDPE film samples were photo-oxidised for 28 days and analysed by ATR-FTIR to compare the

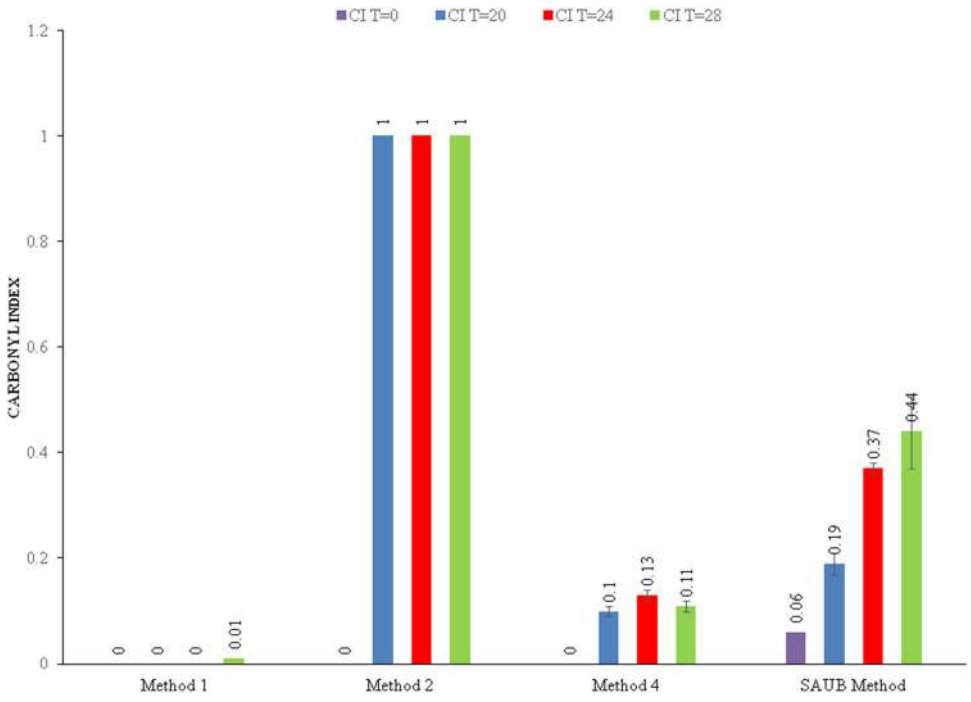

Figure 6: CI data of LLDPE samples at $T = 0$ (purple), 20 (blue l bars), 24 (red) and 28 (green) days of photo-oxidation, using the different methods of calculation listed in Table 3.

different methods of determining CI (Figures 5 and 6). The sampling intervals used to compare the methods were 20, 24 and 28 days of ageing; these intervals were chosen as it was only after 20 days of treatment that the PE samples started showing significant signs of oxidation.

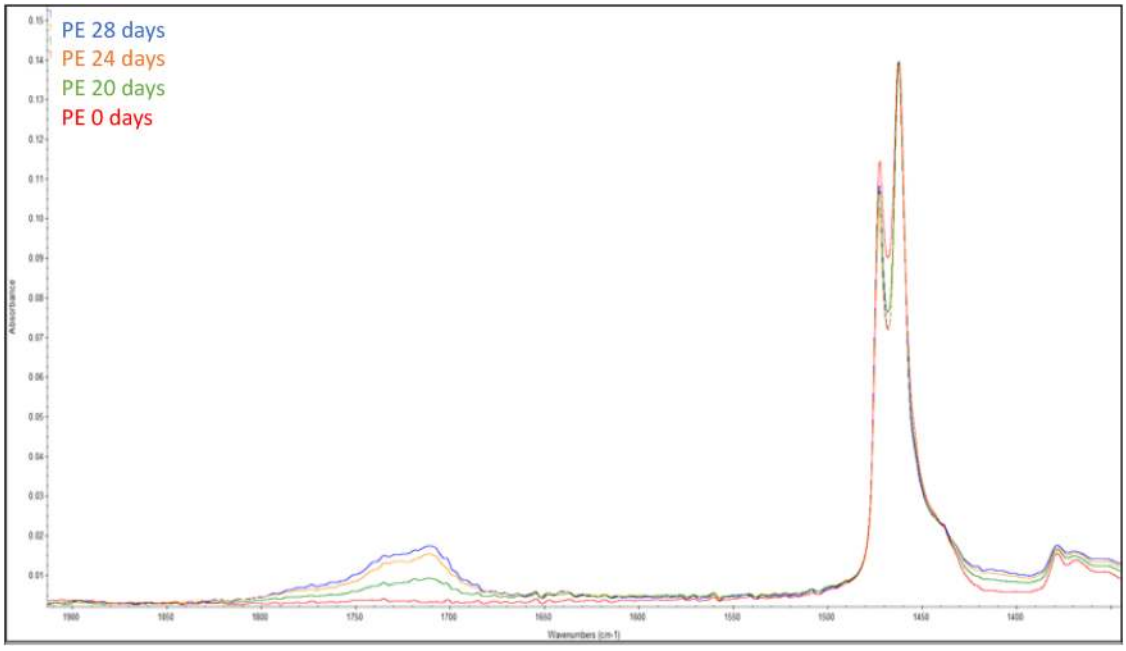

Figure 7: ATR-FTIR spectra in the region of 1,900–1,300 cm^{-1} of a photo-oxidised LLDPE sample showing both C=O and reference peaks after 20 (blue line), 24 (purple line) and 28 (red line) days of exposure. Note: this region was selected for expansion to clearly demonstrate the changes to the carbonyl band over time.

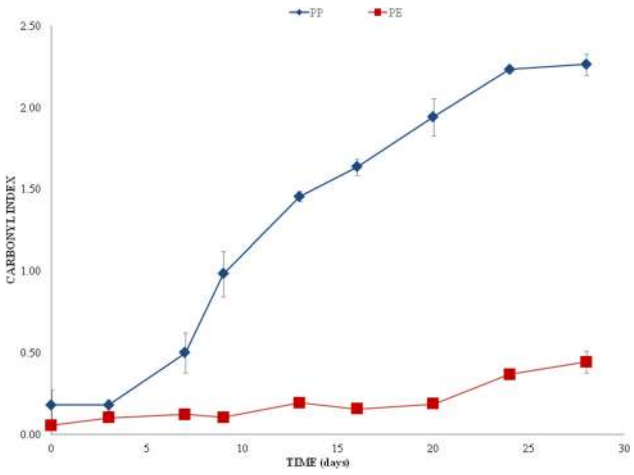

Figure 8: Evolution of CI data using the SAUB method over time for both PP (◊) and PE (□) which have undergone photo-oxidation.

Similar to the PP sample, the spectrum of the photo-oxidised PE sample clearly showed an evolution of the carbonyl region over time (Figure 7); however, this is not represented by all the calculated CI measurements (Figure 5). Method 12 only registered a CI value after 28 days of ageing even though a clear carbonyl peak can be seen at both 20 and 24 days. On the other hand, method 4 calculated the same CI value for all three sample intervals even though it can be seen from the spectra (Figure 6) that this is clearly not an accurate representation of the chemical changes taking place in the carbonyl region. Method 10 also shows inaccuracies in its measurements as it only registers a CI after 24 days and produces the same CI of 0.1 for 28 days. This demonstrates that methods 12, 4 and 10 are not sensitive enough to be able to accurately measure the differences in oxidation which occur for PE over time.

Method 5, which was relatively consistent for calculating the CI for the PP samples, proves to be inconsistent in the case of the PE samples. Using this method gave a lower CI value at 28 days (0.11) compared to a CI of 0.13 at 24 days. This is again unsurprising as focusing solely on the peak height at 1,714 cm^{-1} will bias the CI to the changes in the concentration of ketones, rather than reflecting the changes in all possible carbonyl containing species present.

Finally, the SAUB method revealed CI data consistent with the evolution of the carbonyl band in the ATR-FTIR spectra by taking into consideration both the changes in ketones and the change in concentration of all the carbonyl species, while accurately reflecting this over time. This allows for an accurate correlation of the CI with time to determine the rate and extent of carbonyl functionalisation of the PE. The SAUB method is thus the only measurement method among the other techniques tried that is consistent for both PE and PP samples. This allows for the unique comparison of the change in CI for the same treatment method but within differing polyolefin samples. As an example, we have compared the CI evolution over time for both the PE and PP samples, which have been photo-oxidised, sampled at the same intervals and had the CI calculated using the SAUB methodology (Figure 8).

The SAUB method also allows the picking up of any transitory species that could be produced such as per-acids that are signifiers of oxidation starting, which methods looking at specific peak heights could miss. It is also worth noting that additives added to the polyolefin during the manufacture of the resin can cause interference and introduce error into the measurement. There is the possibility of overlapping bands caused by the presence of slip additives such as erucamide, which can start to appear at around 1,645 cm^{-1}. If multi-reflection ATR were being used, these species would appear much more prevalent and adjustments to the peak area could be necessary to minimise this effect.

Overall, the results demonstrate the advantages of the SAUB CI calculation technique for ATR-FTIR analysis. The PP material, as expected (27), shows a greater degree and a greater relative rate of carbonyl functionalisation over time in comparison to the PE material. These observations fit with the known differences of thermal photo-oxidation associated with the two different polyolefins. The SAUB calculation method allows us to present these relative differences and to calculate that, under the same conditions of accelerated ageing, the PP material had a 2.2-fold increase in the degree of carbonyl functionalisation. In addition, this method of calculation allows us to determine, for the samples tested, that the relative rate of oxidation was nine times faster in PP compared to PE.

4 Conclusion

Our study presents a method of best practice for obtaining CI results by ATR-FTIR using SAUB to evaluate the oxidation of polyolefins over time. This has several key advantages in terms of sample applicability and can be used for both transmission FTIR and ATR-FTIR, to provide a method to best measure CIs. Empirical testing shows the method to have a greater level of sensitivity during the early stages of aging; however, a statistical comparison shows that the results of the SAUB method differ considerably from the other methods. In addition, a result obtained by one method cannot easily be compared to that obtained via another method. For this reason, it is important to standardise the testing methodology used, as this lack of comparability

among CI methods has created a "free-for-all", where a user can pick and choose whichever method proves the outcome they are after, and as has been shown, they often do not provide enough information to independently verify their calculations. Among the benefits of the SAUB method of calculating CI are that it allows for a greater coverage of the C=O band, while still showing correlations for any specific band. It also allows for a general CI to be assessed, where the species present (are largely unknown) and is a good way of reporting general data, while leaving further interpretation open to the investigator. Furthermore, the increased precision the SAUB method appears to provide, allows for greater elucidation of the relative extent and rates of CI, which has the potential to help develop a deeper understanding of the mechanistic aspects of carbonyl functionalisation for polyolefins. Finally, the SAUB technique also allows for the comparisons of different polyolefin materials, which as demonstrated here can be used to gain even greater insights into how one material would perform under a specific set of conditions compared to another over time. What is consistent from the different methods that have been shown is that transmission FTIR spectroscopy works best for PE samples up to around 50 μm, after which it would be best to use ATR-FTIR spectroscopy. To conclude, the adoption of this method would help to reduce confusion and inconsistencies through increasing precision and accuracy in a method capable of allowing relative comparisons of CI to be made between polyolefin materials. With the development of more compact and portable IR machines, this technique offers a beneficial analytical tool for the study of PE and PP, as well as the change in their physicochemical properties, in particular, the relative level of carbonyl species present, whether in the laboratory or in the field.

Acknowledgments: The authors gratefully recognise the financial support of Polymateria, their investors and stake-holders. The authors also wish to thank the work and contributions of Norner AS in the manufacturing of the polyolefin test materials and Dr L. Hill for consultation on statistics tests.

References

(1) Sellin N, Sinezio de J, Campos C. Surface composition analysis of PP films treated by corona discharge. Mater Res. 2003;6:163–6. doi: 10.1016/0014-5793(73)80771-9.
(2) Tuominen M, Lahti J. The effects of corona and flame treatment: part 1. PE-LD coated packaging board. 11th TAPPI Eur PLACE Conf. 2007. p. 15.
(3) Andrady A. Plastics and Environmental Sustainability. Hoboken, New Jersey, USA: John Wiley & Sons; 2015.
(4) Mellor DC, Moir AB, Scott G. The effect of processing conditions on the U.V. stability of polyolefins. Eur Polym J. 1973;9:219–25.
(5) Focke WW, Mashele RP, Nhlapo NS. Stabilization of low-density polyethylene films containing metal stearates as photodegradants. J Vinyl Addit Technol. 2011;17:21–7.
(6) Santos ASF, Agnelli JAM, Trevisan DW, Manrich S. Degradation and stabilization of polyolefins from municipal plastic waste during multiple extrusions under different reprocessing conditions. Polym Degrad Stab. 2002;77:441–7.
(7) Siddiqa AJ, Chaudhury K, Adhikari B. Hydrophilic low density polyethylene (LDPE) films for cell adhesion and proliferation. Res Rev J Med Org Chemistry. 2012;1:43–54.
(8) Renner G, Schmidt TC, Schram J. Chapter 4 – Characterization and Quantification of microplastics by infrared spectroscopy. Compr Anal Chem. 2017;75:67–118.
(9) Andrady AL. Persistence of plastic litter in the oceans. In: Bergmann M, Gutow L, Klages. M, editors. Marine Anthropogenic Litter. Berlin, Germany: Springer Cham; 2015.
(10) Benítez A, Sánchez JJ, Arnal ML, Müller AJ, Rodríguez O, Morales G. Abiotic degradation of LDPE and LLDPE formulated with a pro-oxidant additive. Polym Degrad Stab. 2013;98:490–501.
(11) Antunes MC, Agnelli JAM, Babetto AS, Bonse BC, Bettini SHP. Abiotic thermo-oxidative degradation of high density polyethylene: effect of manganese stearate concentration. Polym Degrad Stab. 2017;143:95–103.
(12) Ali SS, Qazi IA, Arshad M, Khan Z, Voice TC, Mehmood CT. Photocatalytic degradation of low density polyethylene (LDPE) films using titania nanotubes. Environ Nanotechnol Monit Manag. 2016;5:44–53.
(13) Yeh CL, Nikolić MAL, Gomes B, Gauthier E, Laycock B, Halley P, et al. The effect of common agrichemicals on the environmental stability of polyethylene films. Polym Degrad Stab. 2015;120:53–60.
(14) Maalihan RD, Pajarito BB. Effect of colorant, thickness, and pro-oxidant loading on degradation of low-density polyethylene films during thermal aging. J Plast Film Sheeting. 2016;32:124–39.
(15) Elanmugilan M, Sreekumar P, Singha N, De S, Al-Harthi M. Natural weather aging of low density polyethylene: effect of prodegradant additive. Plast Rubber Compos. 2014;43:347–53.
(16) Gulmine JV, Janissek PR, Heise HM, Akcelrud L. Degradation profile of polyethylene after artificial accelerated weathering. Polym Degrad Stab. 2003;79:385–97.
(17) Jakubowicz I, Enebro J. Effects of reprocessing of oxobiodegradable and non-degradable polyethylene on the durability of recycled materials. Polym Degrad Stab. 2012;97:316–21.
(18) Roy PK, Surekha P, Rajagopal C, Chatterjee SN, Choudhary V. Effect of benzil and cobalt stearate on the aging of low-density polyethylene films. Polym Degrad Stab. 2005;90:577–85.
(19) Moldovan A, Patachia S, Buican R, Tierean MH. Characterization of polyolefins wastes by FTIR spectroscopy. Bull Transilv Univ Brasoz Ser I Eng Sci. 2012;5(54):65–72.

(20) Ángeles-López YG, Gutiérrez-Mayen AM, Velasco-Pérez M, Beltrán-Villavicencio M, Vázquez-Morillas A, Cano-Blanco M. Abiotic degradation of plastic films. J Phys Conf Ser. 2017;792:012027.
(21) Tocháček J, Vrátníčková Z. Polymer life-time prediction: the role of temperature in UV accelerated ageing of polypropylene and its copolymers. Polym Test. 2014;36:82–87.
(22) de Carvalho CL, Silveira AF, dos Santos Rosa D. A study of the controlled degradation of polypropylene containing pro-oxidant agents. Springerplus. 2013;2:1–11.
(23) ASTM D5208-14. Standard Practice for Fluorescent Ultraviolet (UV) Lamp Apparatus Exposure of Plastics. West Conshohocken, PA, USA: ASTM Int.; 2014. p. 1–6. www.astm.org.
(24) Antunes MC, Agnelli JAM, Babetto AS, Bonse BC, Bettini SHP, Abiotic thermo-oxidative degradation of high density polyethylene: effect of manganese stearate concentration.
(25) Albertsson A-C, Barenstedt C, Karlsson S, Lindberg T. Degradation product pattern and morphology changes as a means to differentiate abiotically and biotically aged degradable polyethylene. Polymer. 1995;36:3075–83.
(26) Hakkarainen M, Albertsson A-C. Environmental degradation of polyethylene. Adv Pol Sci. 2004;169:177–99.
(27) Ojeda T, Freitas A, Birck K, Dalmolin E, Jacques R, Bento F, et al. Degradability of linear polyolefins under natural weathering. Polym Degrad Stab. 2011;96:703–7.